




Article

Gas-Dependent Reversible Structural and Magnetic Transformation between Two Ladder Compounds

Jun Manabe ¹, Kazuki Nishida ¹, Xiao Zhang ¹, Yuki Nakano ¹, Masaru Fujibayashi ^{1,2}, Goulven Cosquer ^{1,2} , Katsuya Inoue ^{1,2,3}, Seiya Shimono ⁴, Hiroki Ishibashi ⁵, Yoshiki Kubota ⁵ , Misaki Shiga ⁶, Ryo Tsunashima ⁶, Yoko Tatewaki ⁷ and Sadafumi Nishihara ^{1,2,3,8,*} 

- ¹ Department of Chemistry, Graduate School of Science, Hiroshima University, 1-3-1, Kagamiyama, Higashi-hiroshima 739-8526, Japan; m195832@hiroshima-u.ac.jp (J.M.); bmgsmrp.chemistry@gmail.com (K.N.); zhang_x163@163.com (X.Z.); yuki.n.mg.jk@gmail.com (Y.N.); fujiba@hiroshima-u.ac.jp (M.F.); cosquer.goulven@gmail.com (G.C.); kxi@hiroshima-u.ac.jp (K.I.)
- ² Graduate School of Advanced Science and Engineering, Hiroshima University, 1-3-1, Kagamiyama, Higashi-hiroshima 739-8526, Japan
- ³ Chirality Research Center & Institute for Advanced Materials Research, Hiroshima University, 1-3-1, Kagamiyama, Higashi-hiroshima 739-8526, Japan
- ⁴ Department of Materials Science and Engineering, National Defense Academy, 1-10-20 Hashirimizu, Yokosuka, Kanagawa 239-8686, Japan; sshimono@nda.ac.jp
- ⁵ Department of Physical Science, Graduate School of Science, Osaka Prefecture University, Sakai, Osaka 599-8531, Japan; hiroki@p.s.osakafu-u.ac.jp (H.I.); kubotay@p.s.osakafu-u.ac.jp (Y.K.)
- ⁶ Graduate School of Sciences and Technology for Innovation, Yamaguchi University, Yoshida, 1677-1, Yamaguchi 753-8512, Japan; b002wb@yamaguchi-u.ac.jp (M.S.); ryotsuna@yamaguchi-u.ac.jp (R.T.)
- ⁷ Department of Applied Chemistry, Graduate School of Engineering, Tokyo University of Agriculture and Technology 2-24-16, Nakacho, Koganei 184-8588, Japan; ytatewa@cc.tuat.ac.jp
- ⁸ JST, PRESTO, 4-1-8, Honcho, Kawaguchi, Saitama 332-0012, Japan
- * Correspondence: snishi@hiroshima-u.ac.jp

Received: 26 August 2020; Accepted: 17 September 2020; Published: 19 September 2020



Abstract: We report reversible structural transformation that occurs in two ladder compounds: $\text{Cu}_2\text{CO}_3(\text{ClO}_4)_2(\text{NH}_3)_6$ (**1**) and $\text{Cu}_2\text{CO}_3(\text{ClO}_4)_2(\text{NH}_3)_5(\text{H}_2\text{O})$ (**2**), when they are exposed to gaseous vapors. The ladder structures of both **1** and **2** consist of two Cu^{2+} ions and one CO_3^{2-} ion. In **1**, the Cu^{2+} ions are coordinated by three NH_3 molecules on each side, while those in **2** are coordinated by three NH_3 molecules on one side, and two NH_3 molecules and one H_2O molecule on the other side. We demonstrated reversible transformation of **1** and **2** via the exposure of **1** to H_2O vapor and the exposure of **2** to NH_3 vapor using a simple bench-scale method. The minor structural change observed led to a significant difference in physical properties, which we observed using several methods.

Keywords: magnetic property; reversible transformation; spin ladder

1. Introduction

Materials with the capacity to undergo reversible structural and physical changes, usually thermal phase transitions, are required in devices such as sensors and memories [1,2]. Such materials exhibit different structures above and below the phase transition temperature. However, the physical properties of each structure cannot be examined across the entire temperature range. In contrast, light irradiation-induced reversible changes allow for the detailed examination of physical properties throughout the entire temperature range, both before and after the transformation. However, transformation induced by irradiation poses certain problems, like the influence of heat generated

by irradiation and the limited surface area reached by the irradiating light. Therefore, a material that undergoes reversible change in response to an external stimulus other than temperature or light is practically applicable as sensors and memories.

In recent years, spin ladders have attracted significant attention in the field of superconductivity [3–15] due to the theoretical possibility, for an even-leg spin ladder system, to undergo a superconducting transition with doped carriers. In the past, we successfully synthesized two molecular even-leg ladder compounds: $\text{Cu}_2\text{CO}_3(\text{ClO}_4)_2(\text{NH}_3)_6$ (**1**) and $\text{Cu}_2\text{CO}_3(\text{ClO}_4)_2(\text{NH}_3)_5(\text{H}_2\text{O})$ (**2**) [16]. The ladder structure of **1**, $[(\text{H}_3\text{N})_3\text{Cu}-\text{CO}_3-\text{Cu}(\text{NH}_3)_3]_n$ is constructed by alternately stacking two Cu^{2+} ions and one CO_3^{2-} ion, with each Cu^{2+} ion being coordinated by three NH_3 molecules (Figure 1a,b). The ladder structure of **1** is magnetically isolated due to the presence of perchlorate ions between ladders. The temperature-dependent molar magnetic susceptibility of this compound can be reproduced using a magnetically isolated spin ladder model [17], whereby the magnetic exchange interactions of the ladder rung and leg were estimated to be $J_{\text{rung}}/k_B = -364$ K and $J_{\text{leg}}/k_B = -27.4$ K, respectively. Meanwhile, the ladder structure of **2**, $[(\text{H}_3\text{N})_3\text{Cu}-\text{CO}_3-\text{Cu}(\text{NH}_3)_2(\text{H}_2\text{O})]_n$, contains two Cu^{2+} ions and one CO_3^{2-} ion and its structure is similar to that of **1**. One of the two Cu^{2+} ions is, however, coordinated using two NH_3 molecules and one H_2O molecule, thus distinguishing it from **1** (Figure 1c,d). In addition, a small structural phase transition involving the reorientation of the perchlorate ions was observed in **2** at approximately 205 K, thus inducing adjustment in the ladder structure of **2**, without the destruction of the exchange interaction model. The CIF file of **2** at room temperature (HT) is attached to the supplementary materials. The temperature dependence of the molar magnetic susceptibility of **2** was reproduced using an alternating chain model [18], rather than the spin ladder model, with the following magnetic exchange interactions: $J_1/k_B = -7.26$ K, $J_2/k_B = -4.42$ K, and $J_3/k_B = 0$ K. Furthermore, **2** exhibited an antiferromagnetic transition at 3.4 K [19].

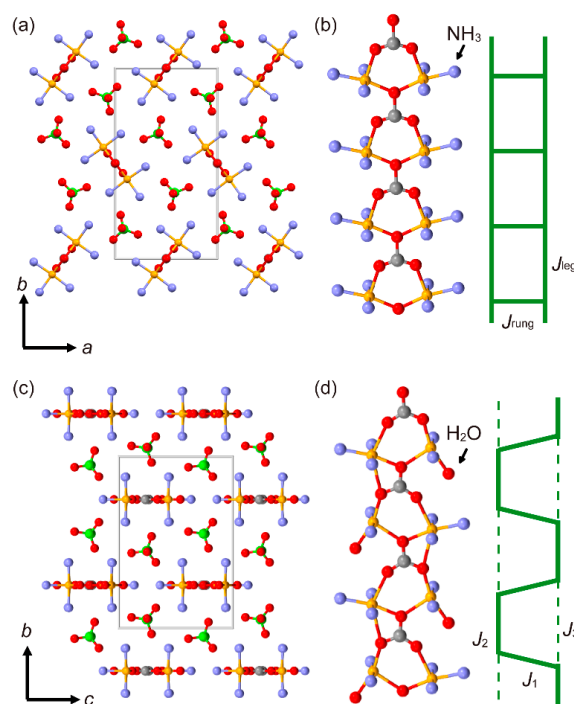
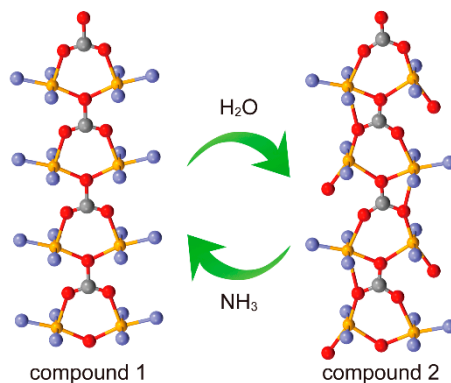


Figure 1. (a) The crystal structure of $\text{Cu}_2\text{CO}_3(\text{ClO}_4)_2(\text{NH}_3)_6$ (**1**), where the Cu^{2+} ions are coordinated on both sides by three NH_3 molecules, observed along the *c*-axis. (b) The ladder structure of **1** and schematic of the ladder configuration with ladder-rung (J_{rung}) and ladder-leg (J_{leg}) magnetic interactions. (c) The crystal structure of $\text{Cu}_2\text{CO}_3(\text{ClO}_4)_2(\text{NH}_3)_5(\text{H}_2\text{O})$ (**2**), where the Cu^{2+} ions are coordinated by three NH_3 molecules on one side and two NH_3 molecules and one H_2O molecule on the other side, observed along the *a*-axis. (d) The distorted ladder structure of **2** and schematic representation of the distorted ladder configuration with the ladder-rung (J_1) and two different ladder-leg (J_2 and J_3) magnetic interactions. (C—grey; N—light blue; O—red; Cl—yellow-green; Cu—yellow).

In the present study, we investigated the reversible structural and magnetic switching between **1** and **2** by exposing the compounds to H₂O and NH₃ vapors, respectively (Scheme 1). Such reversible magnetic switching may be applicable in sensors where they would be used to make distinctions between gases such as NH₃ and H₂O.



Scheme 1. Reversible structural transformation between **1** and **2** via the exchange of H₂O and NH₃.

2. Materials and Methods

Sample preparation: Single crystals of Cu₂CO₃(ClO₄)₂(NH₃)₆ (**1**) and Cu₂CO₃(ClO₄)₂(NH₃)₅(H₂O) (**2**) were synthesized based on past studies [16,20]. Elemental analysis (calcd.) for **1**: C: 2.38 (2.46), H: 3.60 (3.72), N: 16.88 (17.21), and for **2**: C: 2.43 (2.46), H: 3.52 (3.50), N: 13.95 (14.32). To identify structural transformation, powder samples of **1** and **2** were exposed to H₂O or NH₃ vapors, respectively. In this experiment, the powder sample was spread over a glass plate, which was then placed on top of a glass stand inside a beaker containing either H₂O or 14.8 mol dm⁻³ NH₃ aqueous solution (20 mL) in a confined space at 303 K (Figure S1).

Powder X-ray diffraction measurement: Powder X-ray diffraction (PXRD) patterns were measured using a Rigaku RINT2100 diffractometer at r.t. for all samples. The measurements were performed via Cu K α radiation ($\lambda = 1.5418 \text{ \AA}$) at a scanning rate of 2.0° min⁻¹ under an applied electric voltage of 40 kV and a current of 40 mA.

Magnetic measurement: The temperature dependence of the magnetic susceptibility and field-dependent magnetization were measured using a Quantum Design MPMS-5S (Figure 2 and Figure S2), MPMS-XL (Figure S4), and MPMS-3 (Figure S4) superconducting quantum interference device (SQUID) magnetometer using single crystals or powdered samples contained in a gelatin capsule.

Thermal analysis: Thermogravimetric (TG) analyses were carried out on powdered samples using a SII TG/DTA 6200N instrument under N₂ flow. Measurements were conducted at a scanning rate of 5 K min⁻¹. Gas chromatography–mass spectrometry (GC–MS) analyses were performed using a SHIMADZU GCMS-QP2010 Ultra instrument at a scanning rate of 5 K min⁻¹.

Infrared spectroscopy: Infrared spectroscopy (IR) spectra were measured using KBr pellets and a JASCO FT/IR-660 Plus spectrometer within the range of 400–4000 cm⁻¹.

Heat capacities: The heat capacities were measured via the thermal relaxation method using a Quantum Design Physical Property Measurement System (Figure S3).

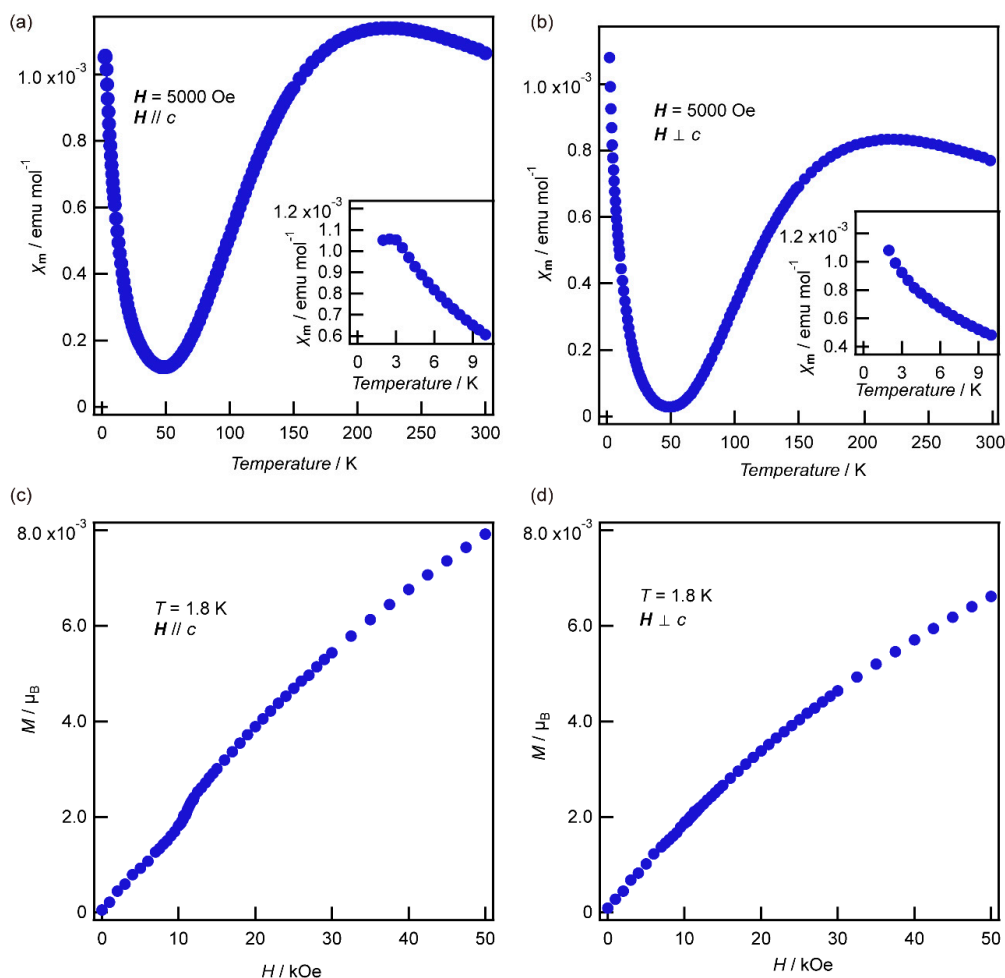


Figure 2. The temperature-dependent molar magnetic susceptibility of **1**, where fields H were applied (a) parallel to and (b) perpendicular to the c -axis. Insets show the plot in the low-temperature range below 10 K. M - H curves for **1** up to fields of 50 kOe, where fields H were applied (c) parallel to and (d) perpendicular to the c -axis at 1.8 K.

3. Results and Discussion

3.1. Magnetic Anomaly of Compound **1**

Magnetic measurements were performed using a single crystal of **1** in magnetic fields H parallel (Figure 2a,c) or perpendicular (Figure 2b,d) to the c -axis. For $H // c$, the temperature dependence of the molar magnetic susceptibility (χ_m - T) of **1** in a field of 5 kOe exhibited unexpected magnetic behavior, hereafter called “anomaly”, at approximately 3 K (Figure 2a). Additionally, a magnetic jump considered to be a spin-flop transition was observed at approximately 11 kOe in the field-dependent magnetization (M - H) curve for **1** at 1.8 K (Figure 2c). When magnetic fields of 3, 11, and 15 kOe were applied at the temperature dependence of magnetization measurements, the magnetic anomaly of the magnetic field of 15 kOe, which was larger than the spin-flop field, vanished (Figure S2). In contrast, such an anomaly was not observed in the χ_m - T and M - H measurements for $H // c$ (Figure 2b,d). Heat capacity measurements were performed in magnetic fields below 30 kOe, parallel to the c -axis, to determine whether the anomaly was attributable to a magnetic phase transition (Figure S3). A peak (partially out of the measured temperature range) was observed below 3 K in the zero-field, and the peak broadened as the magnetic field increased. The results of the magnetic and heat capacity measurements showed that the anomaly of **1** at low temperature was attributable to an antiferromagnetic transition. A similar anomaly in an inorganic spin ladder, whereby an antiferromagnetic transition was detected

in a spin ladder compound doped with magnetic impurities, $\text{Sr}(\text{Cu}_{1-x}\text{Zn}_x)_2\text{O}_3$, was reported by Azuma et al. [21–23]. In the present study, however, **1** was not doped, and the anomaly cannot be explained using this mechanism. To further analyze this phenomenon, we performed magnetic measurements of $H // c$ using a single crystal of **1** exposed to air for 10 days (Figure S4). Under this condition, the peak at 3 K became more prominent. To examine this change, PXRD measurement was performed on **1** after exposing the powder sample to air for 3 days (**1_{air}**). The PXRD pattern of **1_{air}** corresponded to a superposition of the PXRD patterns of **1** and **2** (Figure 3). Because the compositions of **1** and **2** only differ by a molecule (NH_3 or H_2O), these results suggest that NH_3 can be substituted by H_2O from the air in the crystal of **1**. Therefore, the anomaly may not be intrinsic in **1** but in the partial transformation of **1** into **2**.

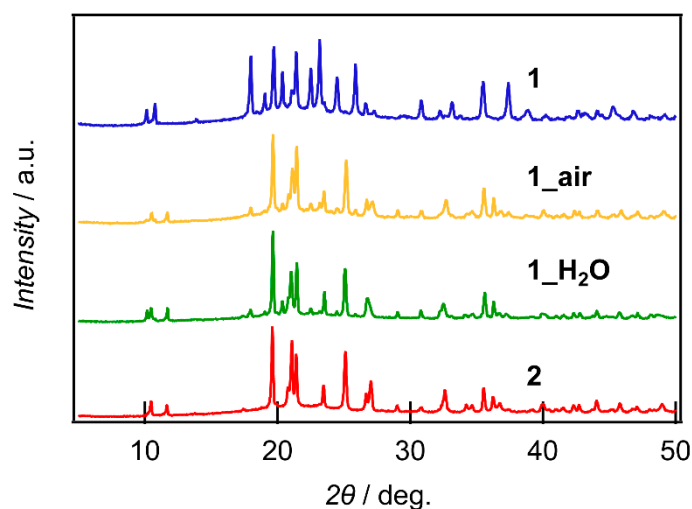


Figure 3. PXRD patterns of **1** (blue), **1_{air}** (**1** exposed to air for 3 days; yellow), **1_{H₂O}** (**1** exposed to H_2O vapor for 4.5 h; green), and **2** (red).

3.2. Transformation from Compound **1** to **2**

To further establish the aforementioned observations and implications, we evaluated the PXRD pattern of **1** exposed to H_2O vapor for 4.5 h (**1_{H₂O}**). The PXRD pattern of **1_{H₂O}** was a superposition of the patterns of **1** and **2** (Figure 3). This implies that in the basic formula $[(\text{H}_3\text{N})_3\text{Cu}-\text{CO}_3-\text{Cu}(\text{NH}_3)_3]$ of **1**, one NH_3 molecule was partially replaced by one H_2O molecule. We confirmed the replacement of the coordinating molecules through TG analysis and GC–MS. Figure S5 shows weight loss in the samples, as well as MS intensity corresponding to the presence of H_2O ($m/z = 18$) across a temperature range of 340 to 450 K. Up to 400 K, the weight loss and MS intensity derived from H_2O was not observed in **1**. In contrast, weight loss was observed in **1_{H₂O}**, and MS intensity derived from H_2O was observed below 400 K. The analysis of **2** yielded results that were similar to those of **1_{H₂O}**. In addition, the elemental analysis of **1_{H₂O}** yielded intermediate values (elemental analysis: C: 2.49, H: 3.68, N: 15.46) between those of **1** and **2** (see the Materials and Methods section). IR spectrum in the $3000\text{--}3700\text{ cm}^{-1}$ region, mainly derived from NH_3 and H_2O ligands, for **1_{H₂O}** is closer to that of **2** than that of **1** (Figure S6). The magnetic behavior of **1_{H₂O}**, as shown in Figure 4b, was drastically different compared to that of **1** (Figure 4a) and tended toward that of **2** (Figure 4c). From these results, we conclude that the NH_3 in **1** was substituted by H_2O after exposure to H_2O vapor, and the anomaly observed in **1** at low temperature was caused by the transformation of **1** to **2** by H_2O , corresponding to the prediction mentioned earlier.

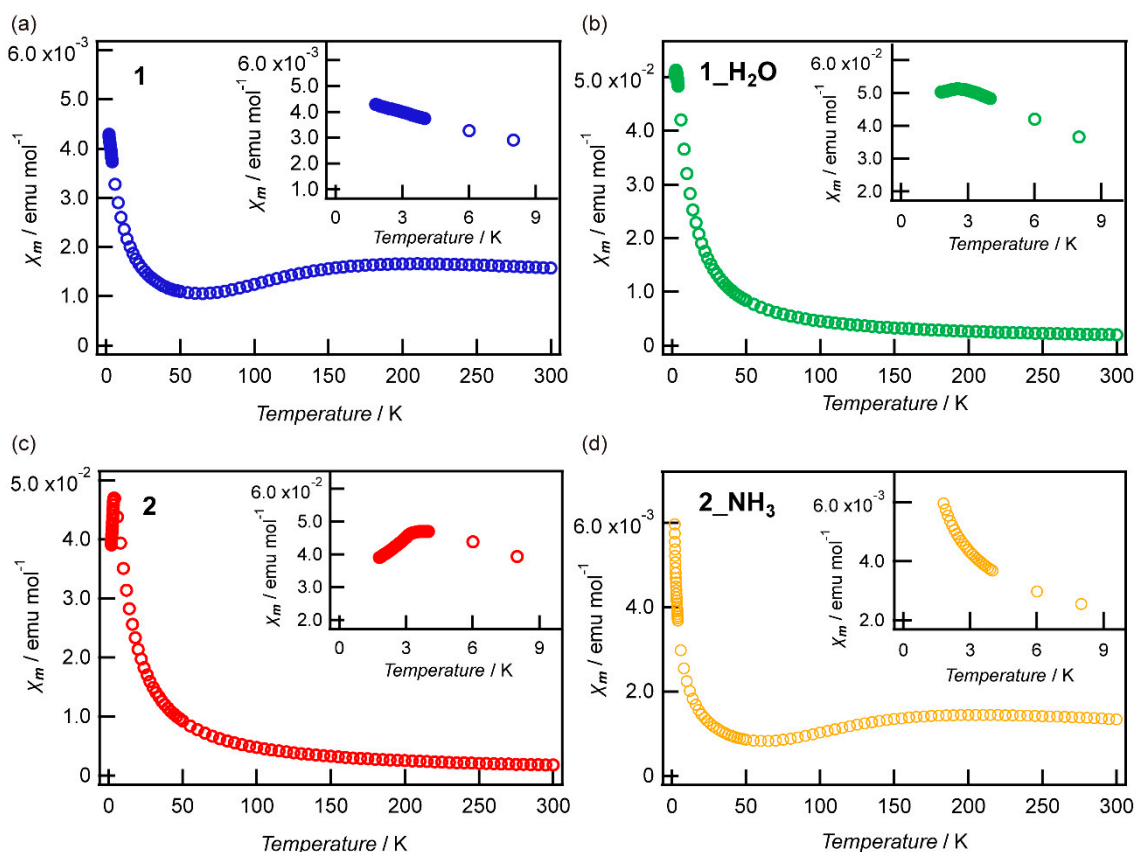


Figure 4. Temperature-dependent molar magnetic susceptibility in an applied field of 5 kOe for (a) **1**, (b) **1_H₂O** (**1** exposed to H₂O vapor for 4.5 h), (c) **2**, and (d) **2_NH₃** (**2** exposed to NH₃ vapor for 2 h). The insets show the data in the low-temperature range (below 10 K).

3.3. Transformation from Compound **2** to **1**

In order to investigate the reverse reaction from **2** to **1**, **2** was exposed to NH₃ vapor from an NH₃ aqueous solution for 2 h (**2_NH₃**). The PXRD pattern of **2_NH₃** exhibited characteristic peaks of both **1** and **2**, implying that the expected transformation had occurred (Figure 5). Therefore, TG analysis and GC–MS were performed for **2_NH₃** (Figure S5). Similar to **1**, the weight loss and MS intensity derived from H₂O was not observed until 400 K. In addition, the results of the elemental analysis of **2_NH₃** also corresponded to intermediate values (elemental analysis: C: 2.68, H: 3.61, N: 16.55) between those of **1** and **2** (see the Materials and Methods section). The IR spectrum of **2_NH₃** in the 3000–3700 cm^{−1} region also changed and was similar to the spectrum for **1** (Figure S6). The results of the magnetic measurements show that the magnetic behavior of **2_NH₃** (Figure 4d) differed from that of **2** (Figure 4c) and approached that of **1** (see Figure 4a). These results indicate that the exposure of **2** to NH₃ vapor transforms it into **1**.

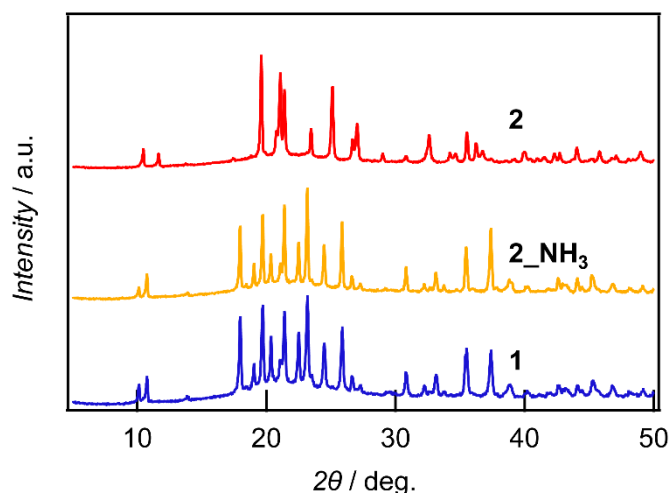


Figure 5. PXRD patterns of **2** (red), **2_NH₃** (**2** exposed to NH₃ vapor for 2 h; yellow) and **1** (blue).

3.4. Reversible Transformation between Compounds **1** and **2**

Reversible transformation between **1** and **2** was investigated. **1_H₂O**, which was obtained by exposing **1** to vapor for 4.5 h, was exposed to NH₃ vapor from an NH₃ aqueous solution for 2 h (**1_H₂O_NH₃**). The PXRD measurement of **1_H₂O_NH₃** was carried out to determine whether the change between **1** and **2** occurred reversibly depending on the gaseous vapors. Figure 6 shows the PXRD pattern of **1_H₂O_NH₃**, including the patterns of **1**, **1_H₂O**, and **2** for comparison. Given that the PXRD pattern of **1_H₂O_NH₃** was similar to that of **1**, we can conclude that **1** and **2** were reversibly changed by gaseous vapors.

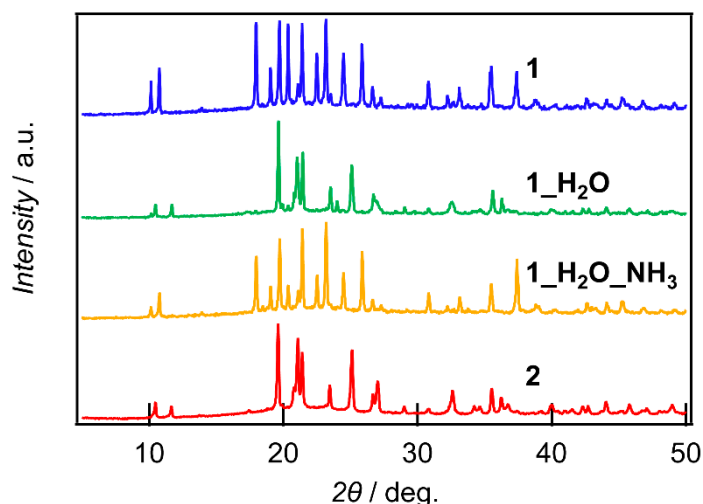


Figure 6. PXRD patterns of **1** (blue), **1_H₂O** (**1** exposed to H₂O vapor for 4.5 h; green), **1_H₂O_NH₃** (**1_H₂O** exposed to NH₃ vapor for 2 h; yellow), and **2** (red).

3.5. Stability of Compounds **1** and **2**

Based on these experiments, the transformation from compound **1** to **2** occurred when **1** was exposed to H₂O vapor, and the opposite transformation from compound **2** to **1** occurred when **2** was exposed to NH₃ vapor, despite the simultaneous presence of H₂O vapor due to the aqueous solution. The results indicated that **1** and **2** were stable in the presence of NH₃ and H₂O vapors, respectively. To verify this, we exposed **1** to NH₃ vapor for 2 h and **2** to H₂O vapor for 4.5 h. The PXRD measurements showed that **1** exposed to NH₃ vapor (**1'**) and **2** exposed to H₂O vapor (**2'**) underwent almost no structural changes (Figure S7). This confirmed that **1** and **2** maintained their original structure when

exposed to NH₃ and H₂O vapor present in the air, respectively. Based on these results, the anomaly observed in the magnetic measurements of **1** at low temperature is assumed to be attributable to a contribution of the antiferromagnetic transition of **2**, produced by the partial transformation of **1** to the more stable structure of **2**, in the presence of H₂O vapor. The transformation did not completely progress to the point where all physical properties were consistent with those of the opposite compound after the transformation, owing to the decomposition of the crystal surface.

4. Conclusions

This study of gas-dependent reversible structural and magnetic transformation between two ladder compounds Cu₂CO₃(ClO₄)₂(NH₃)₆ (**1**) and Cu₂CO₃(ClO₄)₂(NH₃)₅(H₂O) (**2**) was inspired by the observation of an anomaly in a single crystal of **1** at low temperature based on magnetic and heat capacity measurements. Because this anomaly became more prominent after the exposure of **1** to air, we realized that the exposure of **1** to H₂O vapor transformed it into **2**. This transformation was identified using PXRD, TG analyses, GC–MS, elemental analyses, IR spectroscopy, and magnetic measurements. Subsequently, we demonstrated the transformation of **2** to **1** by exposing **2** to NH₃ vapor. We also achieved a reversible transformation between **1** and **2**. In the particular cases where the moisture sensibility of **1** could be avoided or used as advantage, the reversible switching properties demonstrated in our study could allow the development of sensors and memories.

Supplementary Materials: The following are available online at <http://www.mdpi.com/2073-4352/10/9/841/s1>, Figure S1: Experimental setup and schematic diagram, Figure S2: Temperature-dependent magnetization of **1**, Figure S3: Temperature-dependent heat capacity of **1** under variable DC magnetic fields, Figure S4: Temperature-dependent magnetic susceptibility of **1** and **1** exposed to air, Figure S5: TG and GC–MS analysis, Figure S6: IR spectra, Figure S7: PXRD patterns of **1'** and **2'**. Compound2_HT is the CIF file of **2** at room temperature (HT).

Author Contributions: Conceptualization, S.N.; methodology, J.M., K.N., X.Z., Y.N.; validation, J.M., K.N., X.Z., Y.N.; formal analysis, J.M.; investigation, J.M., K.N., X.Z., Y.N., M.S., S.S.; resources, K.I., S.S., H.I., Y.K., R.T., S.N.; data curation, J.M., S.N.; writing—original draft preparation, J.M.; writing—review and editing, M.F., G.C., Y.T., S.N.; visualization, J.M.; supervision, K.I., S.N.; project administration, S.N.; funding acquisition, K.I., S.N. All authors have read and agreed to the published version of the manuscript.

Funding: This research was funded by the Japan Society for the Promotion of Science (JSPS) KAKENHI Grant-in-Aid for Scientific Research, grant number JP19H02799, and the JSPS Core-to-Core Program, Advanced Research Networks. This work was also supported by JST, PRESTO Grant Number JPMJPR19M8, Japan.

Acknowledgments: We thank M. Kubota of the Natural Science Center for Basic Research and Development (N-BARD), Hiroshima University, for performing the elemental analyses. We also thank N. Manada of the Organization for Research Initiatives, Yamaguchi University, for performing the gas chromatography–mass spectrometry analyses.

Conflicts of Interest: The authors declare no conflict of interest.

References

1. Potyrailo, R.A. Multivariable Sensors for Ubiquitous Monitoring of Gases in the Era of Internet of Things and Industrial Internet. *Chem. Rev.* **2016**, *116*, 11877–11923. [[CrossRef](#)]
2. Wuttig, M.; Yamada, N. Phase-change materials for rewriteable data storage. *Nat. Mater.* **2007**, *6*, 824–832. [[CrossRef](#)] [[PubMed](#)]
3. Dagotto, E.; Riera, J.; Scalapino, D. Superconductivity in ladders and coupled planes. *Phys. Rev. B* **1992**, *45*, 5744–5747. [[CrossRef](#)] [[PubMed](#)]
4. Rice, T.M.; Gopalan, S.; Sigrist, M. Superconductivity, Spin Gaps and Luttinger Liquids in a Class of Cuprates. *Europhys. Lett.* **1993**, *23*, 445–449. [[CrossRef](#)]
5. Dagotto, E.; Rice, T.M. Surprises on the Way from One- to Two-Dimensional Quantum Magnets: The Ladder Materials. *Science* **1996**, *271*, 618–623. [[CrossRef](#)]
6. Azuma, M.; Hiroi, Z.; Takano, M.; Ishida, K.; Kitaoka, Y. Observation of a Spin Gap in SrCu₂O₃ Comprising Spin- $\frac{1}{2}$ Quasi-1D Two-Leg Ladders. *Phys. Rev. Lett.* **1994**, *73*, 3463–3466. [[CrossRef](#)]

7. Ishida, K.; Kitaoka, Y.; Asayama, K.; Azuma, M.; Hiroi, Z.; Takano, M. Spin Gap Behavior in Ladder-Type of Quasi-One-Dimensional Spin ($S = 1/2$) System SrCu_2O_3 . *J. Phys. Soc. Jpn.* **1994**, *63*, 3222–3225. [[CrossRef](#)]
8. Azuma, M.; Yoshida, H.; Saito, T.; Yamada, T.; Takano, M. Pressure-Induced Buckling of Spin Ladder in SrCu_2O_3 . *J. Am. Chem. Soc.* **2004**, *126*, 8244–8246. [[CrossRef](#)]
9. Kojima, K.; Keren, A.; Luke, G.M.; Nachumi, B.; Wu, W.D.; Uemura, Y.J.; Azuma, M.; Takano, M. Magnetic Behavior of the 2-Leg and 3-Leg Spin Ladder Cuprates $\text{Sr}_{n-1}\text{Cu}_{n+1}\text{O}_{2n}$. *Phys. Rev. Lett.* **1995**, *74*, 2812–2815. [[CrossRef](#)]
10. Rovira, C. Molecular Spin Ladders. *Chem. Eur. J.* **2000**, *6*, 1723–1729. [[CrossRef](#)]
11. Nishihara, S.; Akutagawa, T.; Hasegawa, T.; Nakamura, T. Formation of a molecular spin ladder induced by a supramolecular cation structure. *Chem. Commun.* **2002**, 408–409. [[CrossRef](#)] [[PubMed](#)]
12. Nishihara, S.; Akutagawa, T.; Hasegawa, T.; Fujiyama, S.; Nakamura, T.; Nakamura, T. Two Polymorphs of (Anilinium)(18-Crown-6)[Ni(dmit)₂]: Structure and Magnetic Properties. *J. Solid State Chem.* **2002**, *168*, 661–667. [[CrossRef](#)]
13. Nishihara, S.; Akutagawa, T.; Hasegawa, T.; Nakamura, T.; Fujiyama, S.; Nakamura, T. Magnetic and ¹H-NMR spectroscopic studies of [Ph(NH₃)](18-crown-6) [Ni(dmit)₂] having molecular spin ladder structure. *Synth. Met.* **2003**, *137*, 1279–1280. [[CrossRef](#)]
14. Ichihashi, K.; Konno, D.; Date, T.; Nishimura, T.; Maryunina, K.Y.; Inoue, K.; Nakaya, T.; Toyoda, K.; Tatewaki, Y.; Akutagawa, T.; et al. Optimizing Lithium Ion Conduction through Crown Ether-Based Cylindrical Channels in [Ni(dmit)₂][−] Salts. *Chem. Mater.* **2018**, *30*, 7130–7137. [[CrossRef](#)]
15. Ichihashi, K.; Konno, D.; Maryunina, K.Y.; Inoue, K.; Toyoda, K.; Kawaguchi, S.; Kubota, Y.; Tatewaki, Y.; Akutagawa, T.; Nakamura, T.; et al. Selective Ion Exchange in Supramolecular Channels in the Crystalline State. *Angew. Chem. Int. Ed.* **2019**, *131*, 4213–4216. [[CrossRef](#)]
16. Zhang, X.; Nishihara, S.; Nakano, Y.; Yoshida, E.; Kato, C.; Ren, X.-M.; Maryunina, K.Y.; Inoue, K. A magnetically isolated cuprate spin-ladder system: Synthesis, structures, and magnetic properties. *Dalton Trans.* **2014**, *43*, 12974–12981. [[CrossRef](#)]
17. Johnston, D.C.; Troyer, M.; Miyahara, S.; Lidisky, D.; Ueda, K.; Azuma, M.; Hiroi, Z.; Takano, M.; Isobe, M.; Ueda, Y.; et al. Magnetic Susceptibilities of Spin-1/2 Antiferromagnetic Heisenberg Ladders and Applications to Ladder Oxide Compounds. *arXiv* **2000**, arXiv:con-mat/0001147.
18. Kahn, O. *Molecular Magnetism*; VCH: New York, NY, USA, 1993.
19. Kobori, S.; Matsui, K.; Kuwahara, H.; Goto, T.; Zhang, X.; Nakano, Y.; Nishihara, S.; Inoue, K.; Sasaki, T. NMR study on the quasi one-dimensional quantum spin magnet with ladder structure. *Hyperfine Interact.* **2016**, *237*, 116. [[CrossRef](#)]
20. Zhang, X.; Nishihara, S.; Nakano, Y.; Maryunina, K.Y.; Inoue, K. A Cuprate Spin Ladder Linked by a Pyridyl Ligand. *Chem. Lett.* **2014**, *43*, 1713–1715. [[CrossRef](#)]
21. Azuma, M.; Fujishiro, Y.; Takano, M.; Nohara, M.; Takagi, H. Switching of the gapped singlet spin-liquid state to an antiferromagnetically ordered state in $\text{Sr}(\text{Cu}_{1-x}\text{Zn}_x)_2\text{O}_3$. *Phys. Rev. B* **1997**, *55*, R8658–R8661. [[CrossRef](#)]
22. Fujiwara, N.; Yasuoka, H.; Fujishiro, Y.; Azuma, M.; Takano, M. NMR Study of Zn Doping Effect in Spin Ladder System SrCu_2O_3 . *Phys. Rev. Lett.* **1998**, *80*, 604–607. [[CrossRef](#)]
23. Ohsugi, S.; Tokunaga, Y.; Ishida, K.; Kitaoka, Y.; Azuma, M.; Fujishiro, Y.; Takano, M. Impurity-induced staggered polarization and antiferromagnetic order in spin-1/2 Heisenberg two-leg ladder compound SrCu_2O_3 : Extensive Cu NMR and NQR studies. *Phys. Rev. B* **1999**, *60*, 4181–4190. [[CrossRef](#)]

